ICANS-XVII
17th Meeting of the International Collaboration on Advanced Neutron Sources
April 25-29, 2005
Santa Fe, New Mexico

The Disk Chopper Spectrometer at NIST: The First Five Years

J. R. D. Copley

NIST Center for Neutron Research, National Institute of Standards and Technology, Gaithersburg, MD 20899-8562, USA

Abstract

The Disk Chopper Spectrometer, at the NIST Center for Neutron Research (NCNR), is a multichopper time-of-flight spectrometer not unlike the IN5 and NEAT spectrometers at the Institut Laue-Langevin and Hahn-Meitner Institut respectively. It is one of the most popular instruments at the NCNR, largely due to its wide range of incident wavelengths and resolution conditions, its large detector coverage, and its ease of use.

1. Introduction

The Disk Chopper Spectrometer (DCS) [1], at the NIST Center for Neutron Research (NCNR), is a direct geometry time-of-flight spectrometer that is used to study a variety of systems ranging from frustrated magnets to proteins in solution. As of this writing (April 2005) it has been operating for nearly five years, during which time we have gained considerable experience and familiarity with the instrument, making improvements as and when required. In this paper we shall review important aspects of the design of the primary spectrometer, and we shall discuss some of the lessons we have learned over the past five years. Too often such lessons are communicated by word of mouth and never written down; we hope that committing these matters to paper (even those that classify as mistakes and may be somewhat embarrassing) will prove useful to current and future designers of neutron scattering instruments.

2. The spectrometer

An overall plan view of the DCS is shown in fig. 1. The primary spectrometer comprises a neutron guide designed as an "optical filter", a cooled crystal filter, a beam shutter, and seven phased disk choppers that deliver clean monochromatic bursts of neutrons to the sample. The secondary spectrometer is nothing much more than an argon-filled flight chamber plus a large array of detectors viewing the sample.

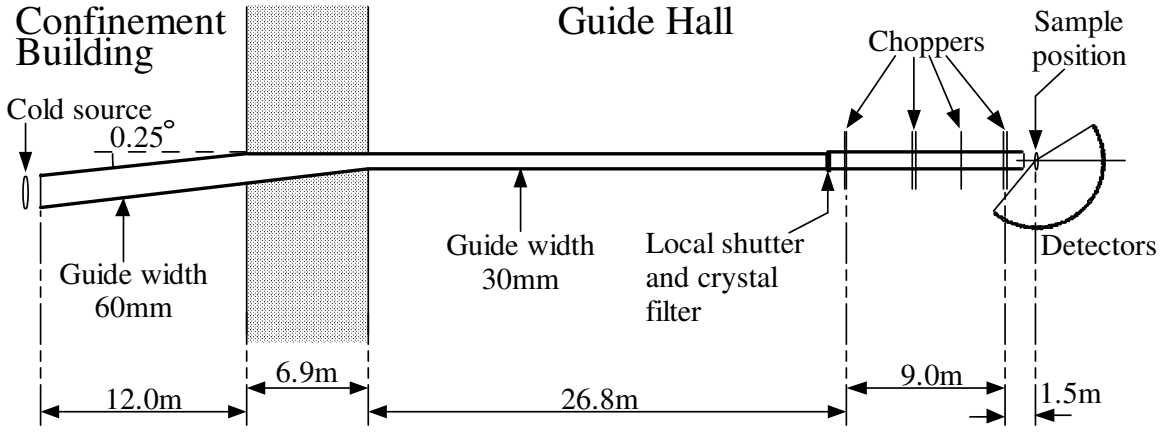

Figure 1. An overall plan view of the DCS. The drawing is to scale in the beam direction.

2.1 Filters

From the start it was deemed important to be able to run the DCS at wavelengths shorter than 4Å (1Å = 0.1nm) and our initial thinking, given that the NIST Cold Neutron Research Facility (CNRF) was designed with straight guides, was to identify a material that could be used as a crystal filter placed in a guide cut in order to remove high energy neutrons and γ-rays. This approach was later shelved for apparent lack of an appropriate material and the concept of an "optical filter" was investigated as a possible alternative. Such a device, as originally described by Hayter [2], is basically a system of two or more straight guides placed end-to-end such that there is no line of sight through the system but high transmission probability for long wavelength neutrons. (Arguably the term should be applied to curved guides but in practice it has the more restricted meaning given.) The final design, illustrated in fig. 1, reduces the width of the guide from 60 mm to 30 mm, introducing an overall angular offset of 0.25°. Its theoretical transmission function, defined as the ratio of neutron *current density* (rather than current) at the exit to current density at the exit of a sufficiently long straight guide, assuming a guide coating with 100% (0%) reflectivity below (above) the critical angle $\theta_C = Q_C\lambda/4\pi$, where the critical wave vector $Q_C \approx 0.026$ Å^{-1} (appropriate to ^{58}Ni) and λ is the wavelength, was expressed as follows in ref. [3]: 100% for $\lambda \geq 4\lambda_C$ where $\lambda_C \approx 1.05$ Å, dropping to 75% at $\lambda = 2\lambda_C$ and 0 for $\lambda \leq \lambda_C$.

Once the guide and the choppers and associated shielding were in place, we collected time-of-flight spectra using a ^{3}He detector placed in the direct beam. The choppers were phased to transmit a single wavelength which produced a sharp peak as expected, but there was an unexpected additional background with significant structure. An example is shown in fig. 2. It turned out [4] that the principal source of the

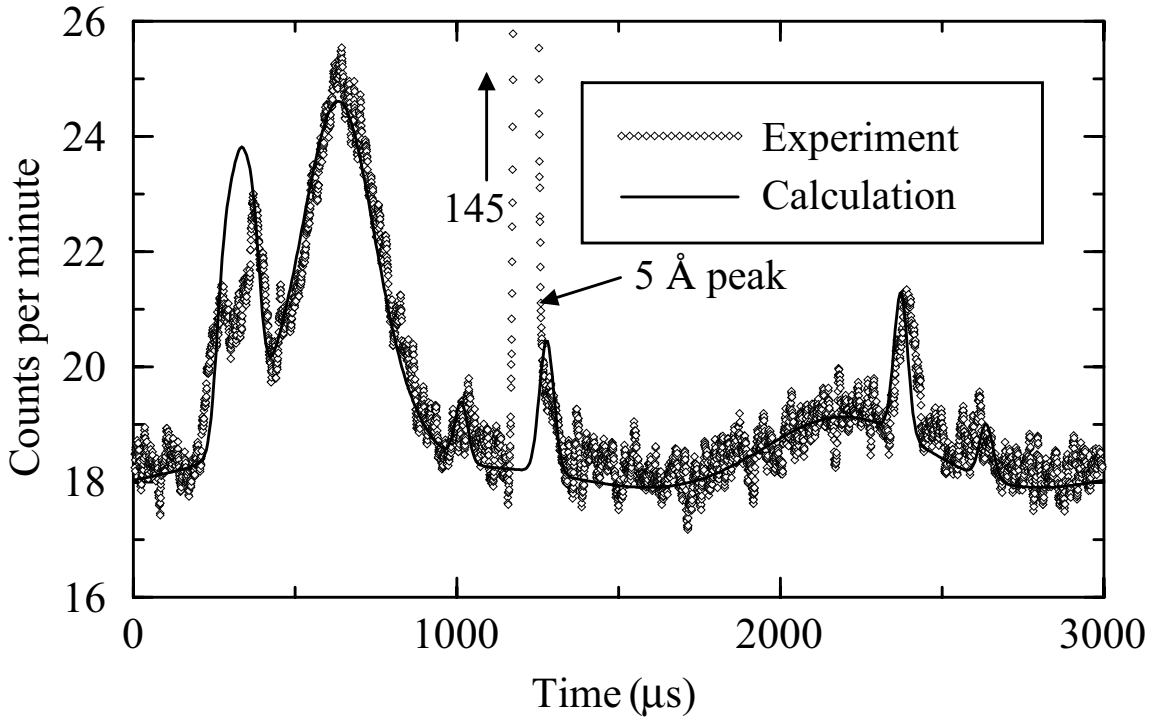

Figure 2. A time-of-flight spectrum obtained with a 3He detector placed in the main beam, 760 mm from the final chopper. The choppers were phased to transmit 5 Å neutrons. The height of the 5 Å peak is 145 counts per minute. The time-dependent backgound is clearly evident. The solid line represents the result of a calculation described in ref. [4]. Note the suppressed zero.

background was neutrons with $\lambda \approx 0.55$ Å (E ≈ 270 meV), reflected by the guide (despite the fact that $\lambda < \lambda_C$), transmitted through an open slot in just one of the choppers, and transmitted through Gd_2O_3 absorbing material (which has very roughly 80% and 10^{-6} transmission per chopper at 0.55 Å and 4 Å respectively) on the remaining six choppers. The sides of the guide, rather than being coated with ^{58}Ni, had been coated with natural nickel plus six Ni-Ti bilayers. The bilayers extend the critical wave vector Q_C to at least that of ^{58}Ni

(≈ 0.026 $Å^{-1}$), but they also produce a peak in the reflectivity at ≈0.04 $Å^{-1}$; this peak is responsible for reflection of the short wavelength neutrons. (We also discovered [4] an error in the earlier calculation [3] of the optical filter's transmission function.)

Having established the source of the background our task was to find a way to remove the short wavelength neutrons responsible for the problem, and since the optical filter was already taking care of high energy neutrons and γ-rays, we revisited the idea of using a pyrolytic graphite (PG) filter. With reference to such a filter, the author had previously stated [3] that "the only windows between 2 and 4 Å are at ~2.34 and ~2.44 Å", but this misrepresents the situation: the significance of these particular wavelengths is that any λ/2 contaminant is very strongly suppressed, but that is irrelevant in the present context because the neutrons to be removed are not second order neutrons from a monochromator but neutrons with a specific narrow range of wavelengths (roughly 0.55±0.10 Å). The measurements of Bergsma and van Dijk [5] suggested that PG would be useful over a wide range of wavelengths, and also showed the advantage of cooling the filter. A PG crystal filter, 110 mm tall, 40 mm wide, 100 mm thick (in the beam direction), and cooled with liquid nitrogen, was accordingly installed a short distance upstream from the beam shutter. Its transmission, derived from pulsed white beam measurements (see section 3.1 below), is shown in fig. 3.

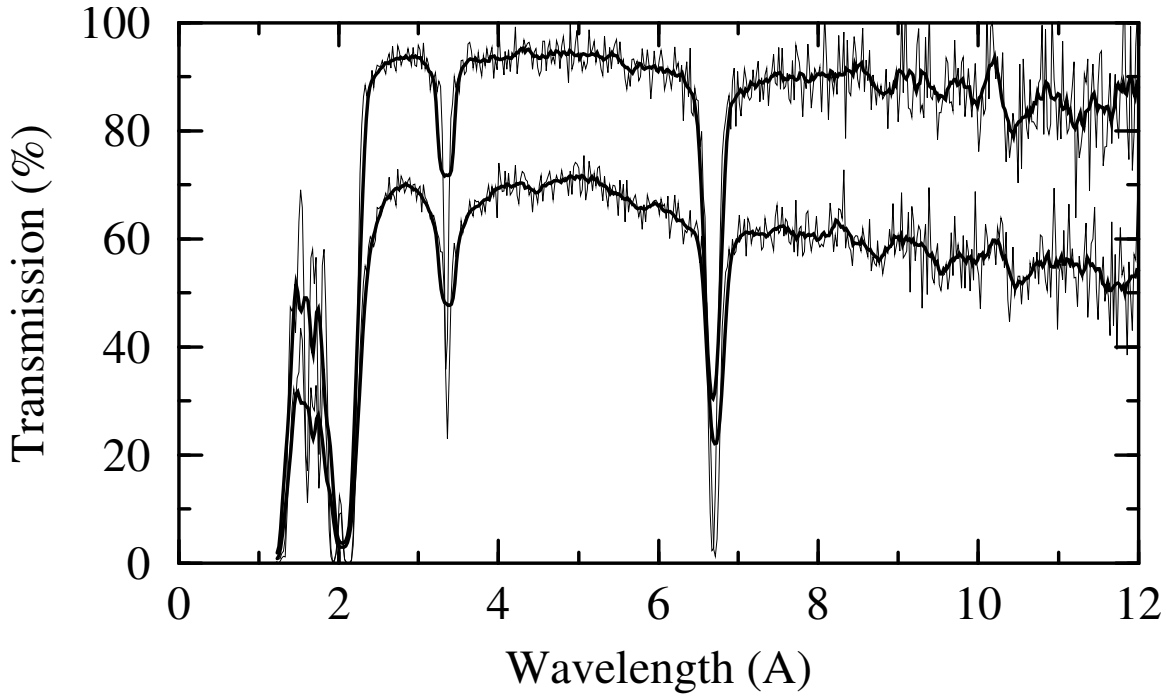

Figure 3. The transmission of the graphite filter, derived from 10-minute white beam measurements with the empty filter cryostat and with the filter at room temperature (lower curves) and cooled with liquid nitrogen (upper curves). The heavy lines represent 10-point running averages of the data.

2.2 Choppers

The conceptual design of the choppers was a major project [6]. The challenge was to design a system that would produce uncontaminated, monochromatic pulses. We also wanted to place multiple slots of different widths on the principal (pulsing and monochromating) choppers in order to be able to change the resolution by changing the width of the beam, without changing the wavelength or the speed of the choppers [7]. The latter requirement implied that we would use counter-rotating chopper pairs [8] to pulse and monochromate the beam.

Having decided that the distance between the first and last chopper pairs would be about 8 m (and the sample-detector distance would be ~4 m), we looked into optimizing the widths of the slots in the principal choppers and the width of the guide. Our conclusion, which was not unexpected, was that there exist optimum values of the ratios of the three widths [9], but this meant that switching among slots of different widths on the principal choppers implied that the width of the guide should also be changed, a task that is easier said than done, given that the choppers would spin at high speed in vacuum, close to an evacuated

guide. As a more practical alternative we developed the idea of a channelled guide, better regarded as a set of nested guides [9], the idea being that the channels restrict lateral beam spread so that (far) fewer neutrons are lost at the downstream choppers when narrow slots are being used.

We also had to think about the design of the counter-rotating choppers: the number of slots, their sizes, and their locations. The problem, given a set of slot widths, was to determine locations such that a counter-rotating pair would produce one (and only one) pulse per revolution in each of its phasing configurations [10]. Ignoring the separation between the two choppers we came up with a design that was communicated to the manufacturer, with instructions to start machining disks to that design. Several weeks later we realized that our neglect of the chopper separation meant that the design would not work because the downstream beam would be contaminated with unwanted additional pulses. Luckily we were able to inform the manufacturer before machining was to start.

Whereas the transmission of an unseparated pair of choppers is independent of the incident neutron wavelength λ, that of a separated pair of choppers depends on λ because the angle β, through which the downstream chopper rotates during the time that a neutron travels the distance between the choppers, is not only proportional to that distance and to the speed of the choppers but to the inverse velocity of the neutron, i.e. proportional to its wavelength. For choppers such as the DCS choppers, separated by 55 mm (the minimum separation acceptable to the manufacturer) and rotating at 20,000 revolutions per minute, β [deg] $\approx 1.67\ \lambda$ [Å]. Since such angles are significant we had to develop a more sophisticated analysis [10].

Key to the analysis was the function $P(\lambda,t)$ which is proportional to the probability that neutrons of wavelength λ are transmitted by a chopper pair at time t. As discussed in ref. [10], this function is not only periodic in t with period T (the rotational period of the choppers) but in λ with period $\Lambda=(h/m)(T/2s)$ where h is Planck's constant, m is the neutron mass, and 2s is the chopper separation. (Negative λ corresponds to neutrons travelling through the chopper pair in the "wrong" direction.) Fig. 4 shows regions in (λ,t) space

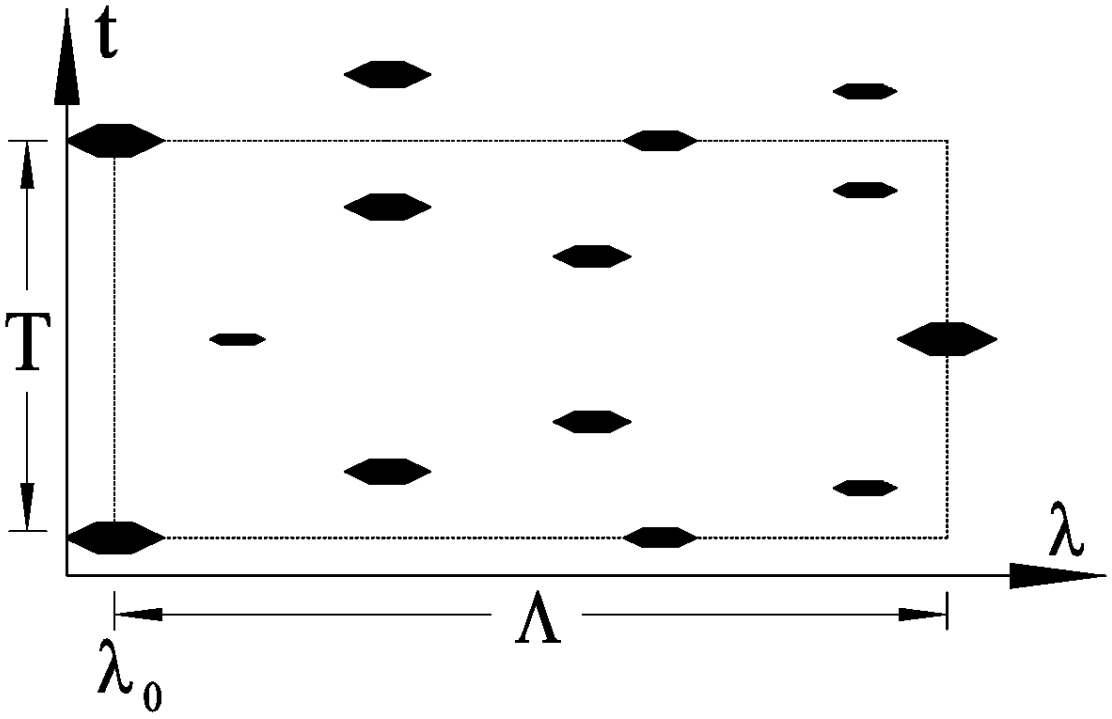

Figure 4. A typical transmission function $P(\lambda,t)$. The function is only nonzero within the shaded areas. The dashed line represents a "unit cell". Unit vectors are $(0,T)$ and $(\Lambda,T/2)$. The intended incident wavelength is λ_0.

where $P(\lambda,t) > 0$, for a specific pair of choppers with three slots of different widths on each chopper. Within the "unit cell" there are nine such regions, corresponding to the nine combinations of slots through which neutrons can pass, as long as they reach the first chopper at an acceptable time with an acceptable wavelength. The ordinate in fig. 4 represents the time that a neutron crosses the mid-plane between the choppers. (The unit cell depicted in fig. 4 has mirror symmetry because the slots happen to be not only identical in width but identically positioned on the two choppers; in general $P(\lambda,t)$ does not have this symmetry.) Fig. 4 is drawn for a particular relative phasing of the choppers, such that the desired neutrons go through the widest slots and the desired wavelength is λ_0. Other relative phasings, corresponding to different choices of wavelength and/or slots in use, are obtained by shifting the system of shaded regions (respecting its periodicity in t and λ) parallel to the λ-axis.

Given a specific relative phasing of the choppers, let us assume (not unreasonably) that the set of shaded regions closest to the t-axis (with the lowest range of wavelengths) represents the desired instrumental setup (choice of wavelength and choice of slots). (We shall only consider relative phasings such that the choice of slots is slots of identical width.) The beam leaving the choppers will be contaminated if the incident beam contained significant intensity in the range of wavelengths corresponding to the set of shaded regions next closest to the t-axis (next lowest in wavelength). Regarding fig.4 as typical, and given that for the DCS $\Lambda \approx 216$ Å (with 2s = 55 mm and T = 3000 μs), it is fair to say that contamination of the type just described will be small. For the design to be acceptable this conclusion must hold for all realistic choices of wavelength and resolution mode.

By carefully choosing the locations of the slots on the pulsing and monochromating chopper pairs we found that we could further reduce the probability of contamination. Slot locations were chosen so that the relatively short contaminant wavelengths transmitted by one chopper pair did not match the relatively short contaminant wavelengths transmitted by the other chopper pair, and vice versa. This increased the wavelength of the shortest wavelength contaminant neutrons that could pass through both chopper pairs, this being a necessary condition for them to reach the sample [11].

Each of the pulsing choppers and each of the monochromating choppers has three slots of different widths (see fig. 1 in ref. [11]). Phasing the chopper pairs to transmit neutrons through the wide, medium width and narrow slots is described as running the spectrometer in "low resolution mode", "medium resolution mode" and "high resolution mode" respectively.

The DCS has two order removal choppers, placed between the pulsing and monochromating chopper pairs. Since their positioning is critical we used more than one approach, including the method of acceptance diagrams [12], to confirm that our choice of positions was fully satisfactory.

In order to minimize frame overlap problems, we also have a frame overlap chopper that operates with the same period as the other choppers (T) or with period mT/(m-1) where $m > 1$ is a small integer (in which case the time between pulses at the sample is mT). The choppers can also be operated with period mT ($m > 2$), but this option is never used. A useful initial rule of thumb, which is perhaps too conservative for low temperature experiments, is that m should be close to λ[Å]/2.

2.3 Secondary spectrometer

The sample chamber, flight chamber and detectors are briefly discussed in ref. [1]. The major conceptual design questions were whether or not the flight chamber should be evacuated and whether or not the detectors should be placed inside the flight chamber. In the end we decided to use a gas-filled flight chamber with the detectors outside the flight chamber. This decision was largely based on considerations of cost, as well as concern to have ready access to the detectors and front-end electronics.

We also had to decide whether to fill the flight chamber with helium or argon and in the end we chose argon (though in principle we could still switch to helium if we wanted to). An advantage of argon is that its scattering cross section (0.68 barns/atom) is half that of helium; a disadvantage is that its absorption is significant (0.38 barns/atom/Å) whereas helium does not absorb neutrons. Our feeling was that absorption should be avoided if possible, but scattering is potentially more problematic since some of it will end up in the detectors. Other considerations included helium's predilection to leak very easily, and argon's ease of handling. We use the boil-off from a 160 liter liquid argon dewar which is replaced every 3 to 4 weeks, with a regular gas bottle as backup.

The engineering design of the sample chamber and flight chamber involved significant challenges, all of which were well met. Indeed the final product exceeded our expectations. We wanted easy access to the sample area, continuous detector coverage over a wide range of scattering angles, and a detector mounting

system that would permit efficient and reproducible installation and removal of the detectors, with all detectors mounted the same known distance from the sample position. In order to achieve continuous detector coverage we wanted continuous inner and outer flight chamber windows. The inner window is made of 0.08 mm aluminum. The outer window was originally made from 0.38 mm Teflon sheet but later replaced with a continuous sheet of 0.009 mm aluminum (see section 3.2 below).

3. Five years' experience

The DCS has been, and remains, a very successful instrument. It has been used for a wide variety of experiments, as the list of DCS-related publications [13] attests. It is also one of the most heavily demanded instruments at the NCNR, largely due to its versatility with regard to wavelength and resolution; plots of intensity and resolution appear in ref. [1] and on the DCS web site [13]. Most people use the low resolution mode and the wavelengths they have used range from 1.8 Å to at least 9 Å. The medium resolution mode, with roughly half the elastic resolution width of the low resolution mode, is occasionally used; in carefully chosen situations the intensity penalty is acceptable in order to access broader ranges in wave vector transfer Q and/or energy transfer E. The high resolution mode, which represents a further halving of the elastic resolution width, has never been used, except for white beam transmission measurements (see below); the intensity penalty is simply unacceptable. This being the case, and given the results of detailed Monte Carlo calculations of the relative merits of different designs for the chanelled guide that runs from the most upstream chopper to the sample chamber [14], the guide was modified in July 2002. Whereas the guide originally had four reflecting channel separator plates, the inner two plates were removed so that the modified guide now has three channels instead of five. Subsequent intensity measurements showed clear gains that met or exceeded the predictions, with no detectable change in the energy resolution nor increase in the background. For further information the reader is directed to ref. [14].

3.1 General remarks

The chopper system was designed, as described in section 2.2, to produce uncontaminated bursts of neutrons over a wide range of wavelengths and in all three resolution modes. To date, no experimental observation has caused us to doubt that the choppers fully meet this requirement.

The DCS has few moving parts and the parts that *do* move, viz. the choppers and the oscillating radial collimator (ORC), perform almost flawlessly. Other systems, such as the flight chamber gas-handling system, the sample stage, and the detectors and data acquisition system, have been almost trouble-free. With regard to the detectors, their inflated rectangular (rather than cylindrical or elliptical) cross section (~31 mm wide, ~12 mm thick) was originally considered critical in order to avoid compromising the energy resolution, particularly when operating in the high resolution mode, but since this mode is not used rectangular geometry is less critical. On the other hand the additional detector width (hence considerably fewer detectors per unit area) and the relatively uniform thickness, as compared with the 25 mm diameter cylindrical starting geometry, can legitimately be regarded as advantages. The down side is that the good (neutron) and bad (noise and γ-ray) contributions to the pulse height spectra are less clearly separated.

Users of the DCS generally like the ease of access to the sample area, both from the side through a large door and from above. A spacious (~31 m^2) mezzanine area, where ancillary equipment is located and sample environments are prepared, is also appreciated. The sample stage includes orthogonal translations in the horizontal plane, elevation, and rotations about three orthogonal axes (sample rotation plus two tilts). All six degrees of freedom have been indispensable, especially when working with single crystals. We use a variety of sample environments that span a wide range of temperatures and magnetic fields. They include extra tall ILL-style ("Orange") cryostats, bottom-loading closed-cycle refrigerators, an 11.5 Tesla superconducting magnet with dilution refrigerator, Helmholtz coils, and a high temperature furnace. Special environments have included gas-loading and high pressure helium experiments combined with one of our standard cryostats. We anticipate a general move toward cryogen-free sample environment equipment for reliability and simplicity of operation. Planned new equipment that fits this description includes a top-loading cryogen-free 4-800 K cryostat optimized for use at the DCS and a 10 Tesla cryogen-free superconducting magnet with an open bore for cryostat inserts. All of these pieces of equipment can be accommodated on the DCS sample stage with the ORC in position; the top of the sample table is nominally 170 mm below the beam center line and the inside radius of the ORC is 200 mm. Because of the restricted space between the ORC and the outer can of some of the more specialized pieces of equipment we have found it extremely useful, indeed indispensable, to be able to lower the collimator ~260 mm in order to be

able to use an appropriate tool to attach the equipment to the sample table. (The ORC is then raised to its normal position for the actual measurements.)

The sample chamber can be filled with a gas such as argon, or with a breathable (80%/20%) mixture of argon and oxygen. The gas enters near the floor and empties to the outside of the building through a port located ~0.66 m above the beam center line. Use of a non-breathable gas is currently considered to be a non-standard procedure requiring prior approval. Since it also takes some time to purge the chamber this option is infrequently employed.

As intimated in the introduction, experiments on many types of materials have been undertaken using the DCS. Perhaps the major surprise has been the large number of magnetism experiments, most of which employ relatively short wavelengths (< 4 Å) and some of which have used single crystals. The breakdown of experiments in FY2004 is as follows: 39% magnetism, 22% materials science, 21% small molecules, 12% biology, 4% complex fluids and 2% polymers. Since the DCS became a regularly scheduled instrument its proposal overload factor has fluctuated between 1.7 and 3.3: in the most recent proposal round it was 2.5.

An unanticipated use of the DCS has been for pulsed white beam transmission measurements on candidate filter materials including assorted boules of bismuth [15] and the pyrolytic graphite that was installed in the filter cryostat (section 2.1). For this type of measurement all but the downstream pair of choppers (closest to the sample) are stopped open, this capability being a particularly useful feature of the chopper control system. The downstream choppers are rotated at a relatively slow speed (typically 2000 revolutions per minute) and phased so that neutrons pass through the narrowest slots (full width 1.35°), and neutrons are counted using a beam monitor situated ~5.55 m downstream from the chopper pair. The slow speed is required because of potential frame overlap problems; at 2000 revolutions per minute one chopper period (30 ms) corresponds to a ~21.4 Å band of wavelengths. The narrowest slots are used in order to achieve good resolution.

A useful advantage of the instrument's continuous detector coverage, from 5° to 140°, and its capability to run at short wavelengths, is that somewhat crude diffraction patterns can be collected fairly quickly: the angular acceptance of each detector is 0.5°. Furthermore the ability to measure elastic scattering from single crystals has been exploited in several measurements such as a recent study of $Pb(Mg_{1/3}Nb_{2/3})O_3$ [16].

3.2 "Spurions"

Notwithstanding the success of the DCS we have occasionally encountered instances where unexpected counts show up in the raw data; in common parlance such events are "spurions".

A problem that the author had not previously encountered occasionally manifests itself (of order once a day) as a questionable data value I(j,k) in a single time channel j and detector channel k. The clue to its origin is that the difference between the observed data value and the expected data value is close to a power of 2, and the explanation is described as a "bit flip": a single bit within the memory of the data acquisition computer is flipped, from 0 to 1 or from 1 to 0. The bit flip is believed to occur during a $^{10}B(n,\alpha)^7Li$ reaction in the borophosphosilicate glass layer, or in the doped silicon area of the memory. The resulting charged particles induce a localized change in the bit state. To correct for this problem we accumulate three histograms as data acquisition proceeds: the normal two-dimensional time-detector histogram I(j,k), and two one-dimensional histograms representing sums over time channel as a function of detector channel and vice versa. Comparing these latter histograms with corresponding sums computed from the two-dimensional histogram *after the measurement* enables us to pinpoint the location and magnitude of the bit flip, and to correct it.

A very different problem appeared during some preliminary measurements with a block of beryllium in the beam, close to the location of the beam shutter. To determine a room background we had placed a spare piece of Gd_2O_3-coated foil in the beam, downstream from the incident beam monitor (which is at the entrance to the sample chamber). We expected to see a low count rate in all detector channels, independent of time channel, but instead we saw an unusual feature at roughly the same time in all detectors (fig. 5). After some false starts we established that this feature was the result of fission neutron production within the beam monitor, presumably followed by partial moderation and then absorption in a ^3He detector. The feature disappeared when the fission chamber was physically removed. The fission chamber was later replaced with a low pressure ^3He monitor that has identical outside dimensions and roughly the same detection efficiency as the fission chamber that it replaced.

Bragg scattering by Teflon has been responsible for several observations of unexpected detector counts. The most notable of these observations occurred during an experiment in 2000. A small peak was observed

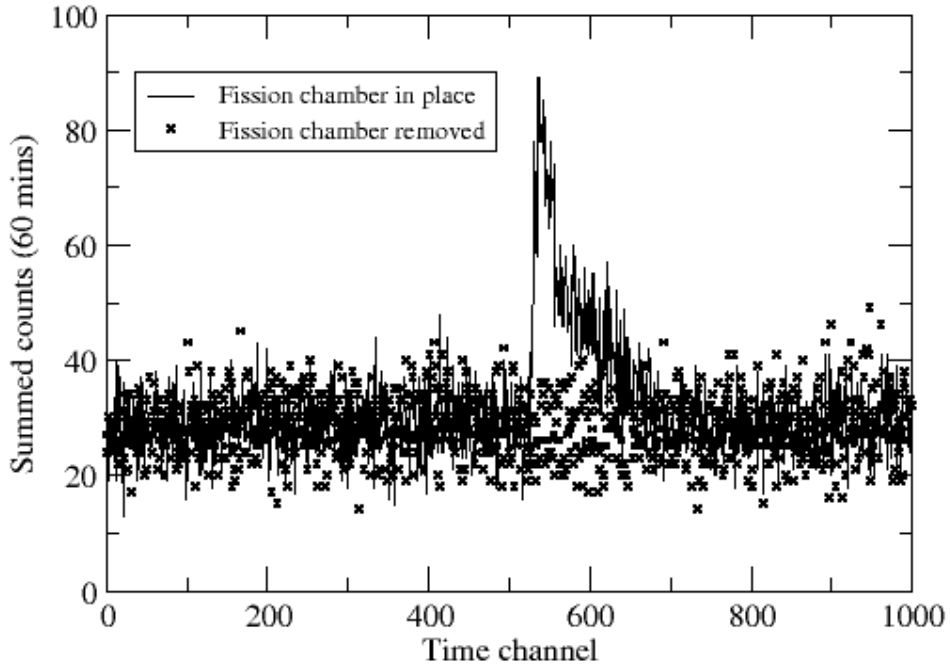

Figure 5. A time-of-flight spectrum obtained with a beryllium block and a Gd_2O_3 foil placed in the beam, with and without a fission chamber in the beam at the entrance to the sample chamber. Counts in one hour, summed over all detectors, are plotted as a function of time channel. The time channel width was 3 μs.

on the long time side of the elastic peak. No peak had been expected, and the absence of a peak on the short time side was inconsistent with detailed balance considerations. The wavelength dependence of the peak's position led us to conclude that we were seeing Bragg scattering by the outer Teflon window of the flight chamber. (The calculated d-spacing was approximately 4.9 Å.) Having checked and double-checked that this was the correct explanation, we replaced the 0.38 mm Teflon sheet with 0.009 mm aluminum as previously mentioned. We have also observed scattering by Teflon insulating material within a beam monitor, and by the Teflon that has occasionally been used to coat the inside surface of an aluminum sample can to protect it from attack by an acidic solvent.

On occasion we have observed scattering by a cadmium beam stop placed a short distance outside the radial collimator. For example, in a measurement using 4.2 Å neutrons we saw three Bragg peaks (002, 100 and 101, with d-spacings of 2.81 Å, 2.58 Å and 2.34 Å, and theoretical relative intensities of 21%, 15% and 100% respectively), together with incoherent scattering at all angles such that the scattering was in reflection and not obstructed by the collimator. If the beam stop is placed just outside the radial collimator such scattering is not observed.

We recently noticed unexpected structure in plots of the scattering function S(Q,E) for a polycrystalline sample. An example (plotted against scattering angle rather than Q) is shown in fig. 6. An examination of the unexpected structure's dependence on wavelength, plus considerable brainstorming, led us to the correct explanation, which is somewhat simplified in what follows. A neutron with wavelength λ, elastically scattered by the sample in the direction of a detector, may with relatively low probability be Bragg reflected by the stainless steel wall of the detector, rather than being absorbed and recorded. For this to happen λ must be such that the Bragg condition for stainless steel can be satisfied and if the Bragg angle is greater than 45° it is quite likely that the neutron will then travel to another detector and be recorded in that detector. The event will occur at a later time and thus appear to be neutron energy loss inelastic scattering. For each possible reflection both the apparent energy loss and the angle between the scattering detector and the most likely absorbing detector can be calculated. Note that the absorbing detector may be

one of several, to the left or to the right of the scattering detector, depending on the azimuthal angle of scattering. To avoid this type of event we should have installed absorbing material between the detectors. Unfortunately we did not, and there is little we can do to circumvent this problem other than to embark upon a fairly significant redesign of the detector mounting system.

From time to time we continue to see spurions, that is to say features in the raw data that we do not understand, and that we believe to be artefacts rather than being associated with what is going on within the sample. Indeed at the time of writing there is at least one recently observed spurion that has so far defied

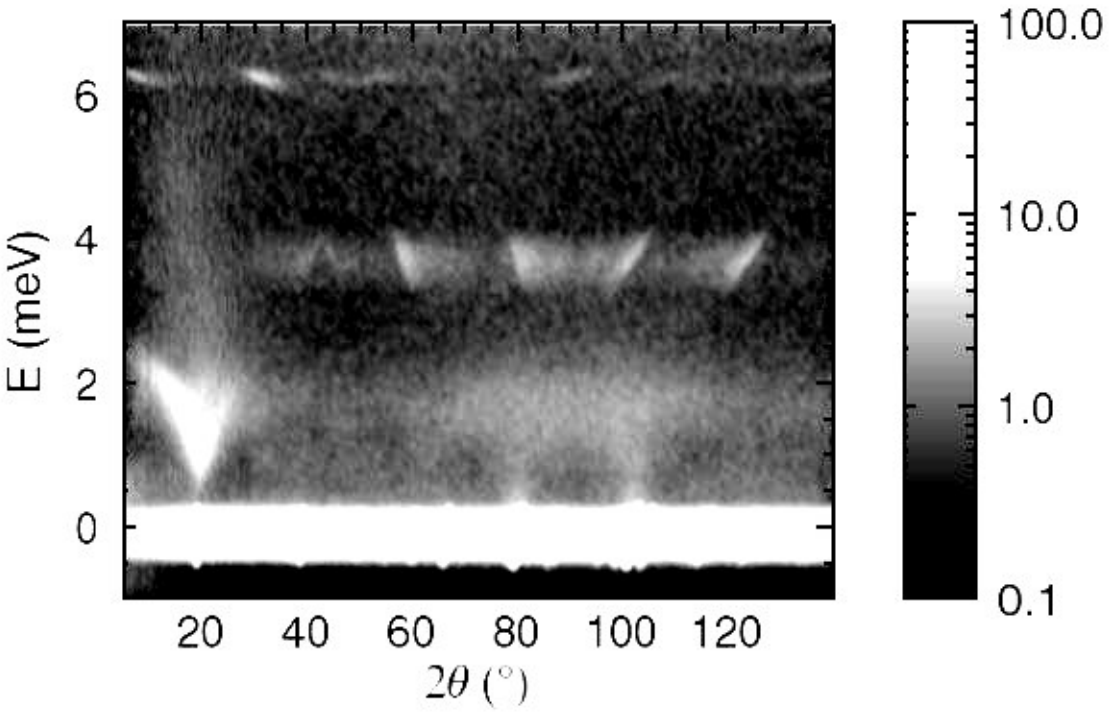

Figure 6. The neutron energy loss results of a measurement on a polycrystalline sample using 3.2 Å neutrons. The abscissa is the scattering angle. The streaks at ~60° and ~100°, with apparent energy transfer ~3.7 meV, are due to powder scattering by the sample at ~80° followed by (111) Bragg reflections from the stainless steel walls of detectors located close to that scattering angle, both to the left and to the right. Similar explanations apply to additional features at 3.7 meV and at 6.3 meV. The latter features are attributed to (200) stainless steel Bragg reflections.

explanation. The confusing aspect of this particular spurion is that it only seems to appear in the upper bank of detectors. (The DCS detectors are organized into three banks centered below, in, and above the scattering plane.) Most of the spurions that we have observed and explained (excluding those described in the second and third paragraphs of this section) involve single or double elastic scattering, and in the latter case at least one of the events is coherent Bragg scattering. Spurions associated with more complicated types of events will surely be more difficult to pin down. An example might be Bragg scattering by a sample and subsequent scattering by the argon in the flight chamber. On the other hand events such as near backscattering by the outer vacuum vessel of a cryostat or closed cycle refrigerator unit, and subsequent scattering by the sample, may well occur. An unfortunate consequence of the popularity and pressure for time on the DCS is that we do not have the luxury to engage in a comprehensive and potentially time-consuming investigation whenever a spurion is suspected. In the author's humble opinion it is unlikely that Monte Carlo simulations of "complete" instruments will be useful as a means to help us understand or predict some of the more elusive spurions that are bound to appear in future instruments, especially when backgrounds are low.

The next five years

The imminent commissioning of next generation sources such as the United Stated Spallation Neutron Source clearly has implications for the future of reactor-based time-of-flight instruments such as the DCS. We believe that the DCS will remain popular and productive for a number of years. We plan to replace the chopper control elecronics and perhaps make improvements to the data acquisition system. Other possibilities include changes to the neutron guide, using guide coatings with higher critical wave vector and perhaps incorporating novel focussing concepts. If a converging guide is installed we may also need to modify the design of the chopper disks.

Acknowledgements

I am grateful to current and former DCS colleagues for numerous helpful discussions. They include Craig Brown, Inmaculada Peral, and Yiming Qiu. I particularly thank Jeremy Cook for his advice and assistance over the years. I am also indebted to Christoph Brocker for his excellent engineering design of the DCS sample chamber, flight chamber and detector mounting system, to Don Pierce for his skilled design of the neutron guide, including the vacuum interface to the chopper housings, to Terrence Udovic, Gregory Downing, and Felix Altorfer for assistance, and to Ruep Lechner for advice and encouragement. John Larese is thanked for the long-term loan of an ILL-style ("Orange") cryostat. This work was supported in part by the National Science Foundation under Agreement No. DMR-0086210.

References

[1] J. R. D. Copley, J. C. Cook, Chem. Phys. **292**, 477 (2003).
[2] J. B. Hayter, in *Neutron Optical Devices and Applications* (Proceedings SPIE **1738)**, edited by C. F. Majkrzak and J. L. Wood (Bellingham, Washington, 1992), p. 2.
[3] J. R. D. Copley, J. Neut. Res. **2**, 95 (1994).
[4] J. R. D. Copley, J. C. Cook, Physica B **283**, 386 (2000).
[5] J. Bergsma, C. van Dijk, Nucl. Instr. And Meth. **51**, 121 (1967).
[6] J. R. D. Copley, in *Proceedings of a Workshop on Methods for Neutron Scattering Instrumentation Design* (E.O. Lawrence Berkeley National Laboratory Report No. 9609353) (LBNL-40816, UC-404), edited by R. P. Hjelm (Berkeley, California, 1997), p. 94.
[7] R. E. Lechner, private communication.
[8] P. A. Egelstaff, in *Proceedings of the International Conference on the Peaceful Uses of Atomic Energy, Geneva, 1955*, vol. 4 (United Nations, New York, 1956), p. 70.
[9] J. R. D. Copley, Nucl. Instr. Meth. A **291**, 519 (1990).
[10] J. R. D. Copley, Nucl. Instr. Meth. A **303**, 332 (1991).
[11] J. R. D. Copley, Physica B **180 & 181**, 914 (1992).
[12] J. R. D. Copley, J. Neut. Res. **1**, 21 (1993); J. R. D. Copley, Nucl. Instr. Meth. A **510**, 318 (2003).
[13] http://www.ncnr.nist.gov/instruments/dcs/.
[14] J. C. Cook, J. R. D. Copley, Rev. Sci. Instrum. **75**, 430 (2004).
[15] T. J. Udovic, D. A. Neumann, J. Leão, C. M. Brown, Nucl. Instr. Meth. A **517**, 189 (2004).
[16] G. Xu, G. Shirane, J.R.D. Copley and P.M. Gehring, Phys. Rev. B**69**, 064112 (2004).